A Common Mechanism Underlies the Dark Fraction Formation and Fluorescence Blinking of Quantum Dots

Nela Durisic,[†] Paul W. Wiseman,[†,‡,*] Peter Grütter,[†,*] and Colin D. Heyes[†,§,*]

[†]Department of Physics, McGill University, 3600 Rue University, Montreal, Quebec, Canada, H3A 2T8, and [‡]Department of Chemistry, McGill University, 845 Rue Sherbrooke, Montreal, Quebec, Canada, H3A 2K6. [§]Present address: Department of Chemistry and Biochemistry, University of Arkansas, 345 N. Campus Drive, Fayetteville, AR 72701.

ABSTRACT CdSe quantum dots (QDs) are known to exhibit both power-law blinking dynamics and a dark fraction. A complete description of the mechanistic origins of these properties is still lacking. We show that a change in the pH of the QD environment systematically changes both the dark fraction and the blinking statistics. As pH is lowered, shorter "on" times and longer "off" times, as well as an increase in the permanent dark fraction, are observed. The increase in the dark fraction is preceded by a decrease in the emission intensity of a single QD. Interestingly, the form of the probability distribution function describing blinking changes when the QDs are taken from an air-exposed environment into an aqueous one. These results are used to propose a coupled role for H^+ ions by which they first reduce the intensity of the emitting state as well as affect the probabilities of the QD to switch between "on" and "off" states and eventually trap the QD in a permanent "off" state. We discuss and extend two theoretical blinking models to account for the effect of H^+ ions as well as to highlight their common principle of a diffusion-controlled mechanism governing blinking.

KEYWORDS: intermittency · nanoparticle · TIRF microscopy · power-law dynamics · hole trapping · energy diffusion

It has been known for over a decade that quantum dots (QDs) exhibit fluorescence blinking with power-law statistics over several orders of magnitude in time.[1−3] However, a complete understanding of the physical mechanism underlying this phenomenon has remained elusive. Several models have been proposed to explain the temporary dark ("off") state including tunneling of a charge carrier from the excited QD to an external trap state[4−6] or trapping at sites internal to the QD, particularly at the surface.[7−9] In principle, power-law dynamics can be explained by a model containing static trap sites for the charge carriers,[3,10] but in order for QDs to be "on" long enough to be observed by fluorescence at the single QD level, a trap state must lie close to the QD. This would then lead to exponential blinking dynamics for these observed QDs (see the recent review by Cichos *et al.*[11] for a more complete discussion). Thus, to observe long "on" times with power-law dynamics at the single QD level, there must be a stochastically fluctuating component to the mechanism, such as fluctuations in the energy and/or position of the external trap sites[5] or fluctuations of energy levels within the QD.[8,12]

Various observations have been made which lend support to one or another of these models. Issac *et al.* observed that blinking of CdSe−ZnS core−shell QDs is correlated to the dielectric constant of the environment surrounding the QDs,[6] which was interpreted with the view that the traps are external. Krauss and Brus used STM to show that blinking is associated with the QD adopting a positive charge, indicative of electron ejection.[4] However, Pelton *et al.* found that blinking statistics are independent of the external environment, seeding doubt in the external trap model.[13] Heyes *et al.* later observed that the blinking of CdSe−ZnS core−shell QDs is independent of the shell thickness,[9] which added to the uncertainty in the external trap model. These observations are consistent with a model in which the holes are trapped at the electron-rich surface of the QD or at the core−shell interface for the case of core−shell QDs.[7−9] Subsequent experiments on CdSe−Cd_xZn_yS core−multishell QDs with very thick (18 monolayers) and highly crystalline shells have revealed that blinking can be suppressed.[14] Similar experiments on CdSe−CdS core−shell QDs, also with very thick and highly crystalline shells, showed reduced blinking.[15] The key to these studies is the reduced lattice strain between the core and shell compared to the more commonly used ZnS shell material together with the thickness and high crystallinity of the shell, suggesting that trap sites can exist in the shell at crystal defects or at the core−shell interface.[9]

*Address correspondence to cheyes@uark.edu, paul.wiseman@mcgill.ca, peter@mail.mcgill.ca.

Received for review October 14, 2008 and accepted April 14, 2009.

Published online April 22, 2009.
10.1021/nn800684z CCC: $40.75

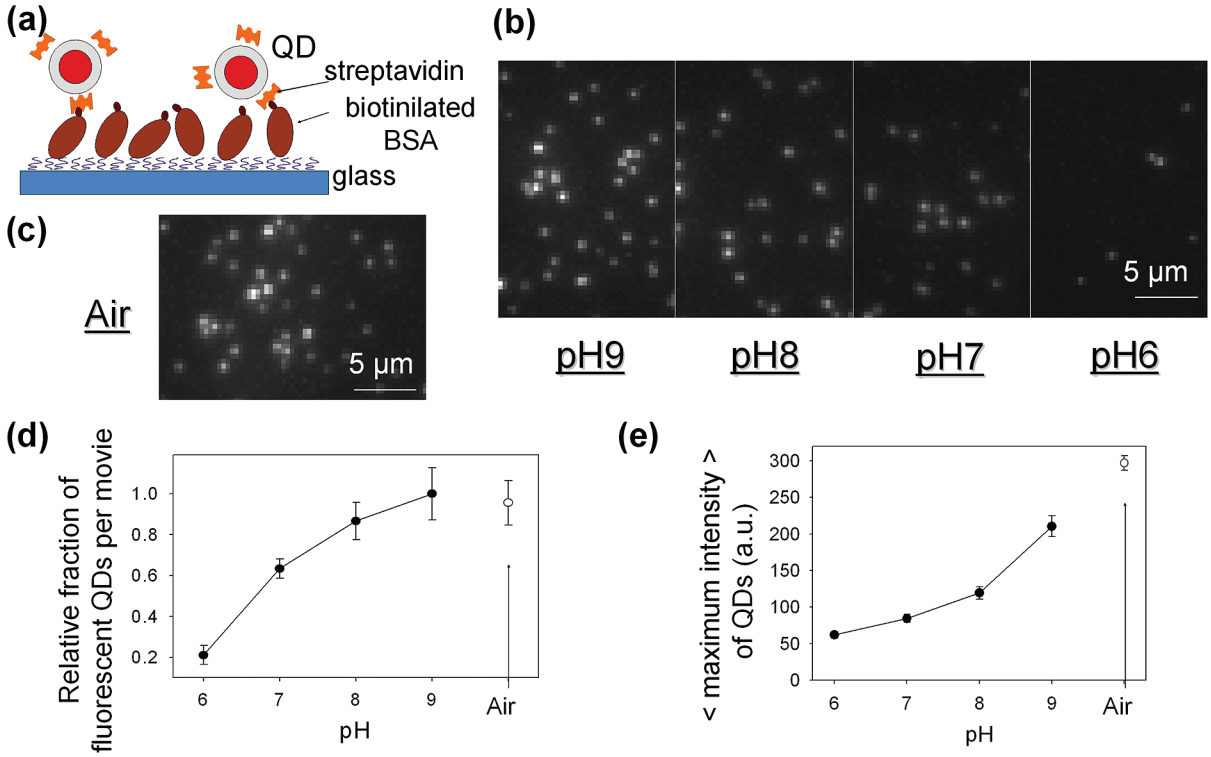

Figure 1. (a) Schematic representation of the immobilization of streptavidin-functionalized core−shell QDs onto biotinylated BSA-coated glass surfaces. (b) Fluorescence microscopy maximum intensity projection images of QDs as a function of pH. Each image is formed by displaying the maximum intensity of each pixel from each frame of a 2000 frame image series. (c) Fluorescence microscopy image of QDs in air as a comparison to those under different pH buffer conditions. (d) Quantification of the relative number of fluorescent QDs as a function of pH (normalized to 1 at pH 9) to determine the effect of pH on the dark fraction. (e) Average of the maximum intensity of each QDs in the "on" state as a function of pH.

Recently, Pelton *et al.* measured the power spectral density of fluctuations and extended the time scale of blinking observations to the microsecond scale.[16] They observed a change in the blinking behavior below a critical time of a few milliseconds, supporting a diffusion-controlled blinking model with the critical time depending on the characteristic diffusion time on the energy surface. In contrast, Sher *et al.* found that the blinking behavior of QDs is the same on the nanosecond time scale and on the hundred millisecond to second time scale,[17] and FCS experiments have shown similar behavior on the microsecond time scale,[10] implying that the blinking dynamics is unchanged across many orders of time. Chemical effects on the QD blinking have also been reported, but with conflicting observations. Hohng and Ha reported that blinking of core−shell QDs can be suppressed by the thiolated molecule, β-mercaptoethanol (BME),[18] while Kramm and co-workers reported that blinking was not suppressed by BME, but that the fluorescence intensity of single QDs was reduced.[19] In fact, the effects of thiolated molecules on the fluorescence properties of QDs were shown to be very complex.[20,21] Fomenko and Nesbitt recently observed that blinking can also be suppressed by the presence of propyl gallate.[22] The presence of electron-donating moieties such as oligo(phenylene vinylene),[23] mercaptoethylamine,[24] and dopamine[25] was shown to influence blinking. One study revealed that the intensity of the "on" state switches between different levels, with each level showing a different fluorescence lifetime.[26] An earlier theoretical paper had proposed the existence of various "on" state intensities based on the presence of localized external charges near the surface of the QD.[27] These apparently conflicting effects highlight the need for further experimental studies and theoretical development to understand the blinking mechanism more thoroughly.

Another surprising observation was made in 2002 by Ebenstein and Banin.[28] Simultaneous AFM and fluorescence microscopy identified that a given sample of surface-immobilized QDs contains a fraction of dark particles—a subpopulation of QDs that are nonfluorescent. A similar experiment using QDs with a different surface functionalization highlighted the ubiquitous nature of the effect.[29] The dark fraction was also shown to exist for QDs in solution, demonstrating that the observed effect was not a result of the surface immobilization.[30] A significant fraction of dark particles was also found by photothermal detection.[31] Additionally, the single particle quantum yield was shown to be very different from the ensemble quantum yield,[28,32] and the ensemble quantum yield was found to be correlated largely to the dark fraction.[30] Heyes *et al.* later showed that the "on" state average intensity was only slightly higher for higher quantum yield QDs,[9] supporting the

idea that the dark fraction plays a major role in determining the ensemble quantum yield.

In this study, we analyze the blinking statistics and the dark fraction of QDs as a function of pH. We show that reducing the pH of the solution surrounding the QDs from 9 to 6 changes both the blinking statistics and the dark fraction in a systematic way, which suggests a coupled role of H^+ ions in the underlying mechanism. From these observations, we propose a model by which the H^+ ions interact with the QD, changing the number and/or energies of trap states, which first change the blinking dynamics and then affect the dark fraction.

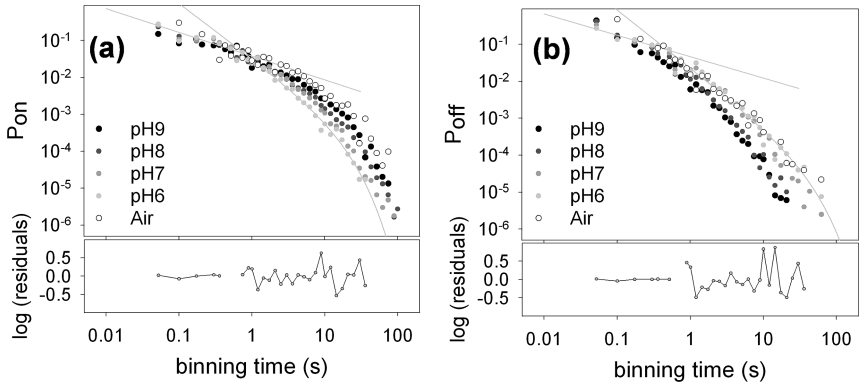

Figure 2. (a) Probability distributions of observing "on" events of a particular duration as a function of pH and in air. (b) Probability distributions of observing "off" events of a particular duration as a function of pH and in air.

RESULTS

Figure 1a schematically depicts the experimental immobilization of streptavidin-functionalized QDs to a biotinylated glass surface. Immobilization is necessary for the water-soluble QDs so that blinking can be observed for long time periods as aqueous buffer solutions were placed over the samples and would otherwise wash them away from the surface. In order to check that the presence of the BSA surface did not affect the blinking dyanmics, we performed the experiment by adsorbing the QDs to bare glass. The results were identical with the exception that analysis was complicated by the fact that many of the soluble QDs were washed away from the surface by the addition of buffer. Figure 1b shows maximum intensity projection images as a function of pH calculated from image series of 100 s for fluorescent CdSe QDs (taken from different areas of the same sample). For comparison, a projection image of fluorescent QDs for a sample in air is also presented (Figure 1c). Figure 1d plots the relative number of fluorescent QDs present on the surface as a function of pH and in air (normalized to 1 at pH 9). It is clear that the dark fraction significantly increased as pH is lowered from 9 to 6 (at pH 5, no fluorescent QDs were visible). Furthermore, there is virtually no difference between the number of fluorescent QDs observed in air and at pH 9, suggesting that OH^- ions have a negligible effect on the dark fraction compared to H^+ ions and that a concentration of H^+ ions of 10^{-9} M is too low to have an effect. Figure 1e presents the maximum "on" state brightness averaged over many QDs as a function of pH. There is a clear trend for the QDs in the "on" state toward lower emission intensity as pH is lowered from 9 to 6.

To ensure that the QDs were not washed away by the various pH-buffered solutions, AFM was used to image the same QDs upon exposure to different pH buffers. These data are presented in the Supporting Information (Figure S1). The QDs remained bound to the surface after changing buffer solutions, providing clear evidence that the reduction in the number of observed fluorescent QDs in Figure 1 is related to the change in the dark fraction and is not the result of the unbinding of the QDs upon change of solution.

The probability to observe "on" or "off" events of a given time duration as a function of pH is presented in Figure 2a,b, respectively. There is a clear trend toward observing shorter "on" events and longer "off" events as the pH is lowered. The probability distributions have complex shapes, and we attempted to fit the data to several functions based on a number of models in the literature. These included single power law,[3] exponential,[10] single power law with exponential cutoff,[2,9,12] as well as a stretched exponential funtion. A power law with exponential cutoff is found to fit the data well at longer time durations, as has been observed previously for "on" times,[2,9] but we also observe it here for "off" times on approximately the same time scales. Additionally, at short binning times (<1 s), a second power-law behavior is evident for both "on" and "off" times. This additional behavior only occurs for samples exposed to pH solution and not for those in air. A recent paper by Pelton *et al.*[16] also observed the change in power-law exponent at faster time scales and fit the fast time scale region with one power law (when $t \ll t_c$) and fit the slower time scales region with a different power law (when $t \gg t_c$). By using this fitting method, we were able to obtain excellent fits to our experimental data at the various pH values. Recent theoretical and experimental papers have discussed the possible origins of this short time scale behavioral change in the framework of a diffusion-controlled mechanism underlying the blinking process.[12,16,33]

Intermittent diffusion of the energy levels across a certain boundary defining the transition from an "on" to an "off" state, solved as a first-passage time problem, yields a power-law probability density function for blinking in the form[8,12]

$$P(t) \propto t^m \qquad (1)$$

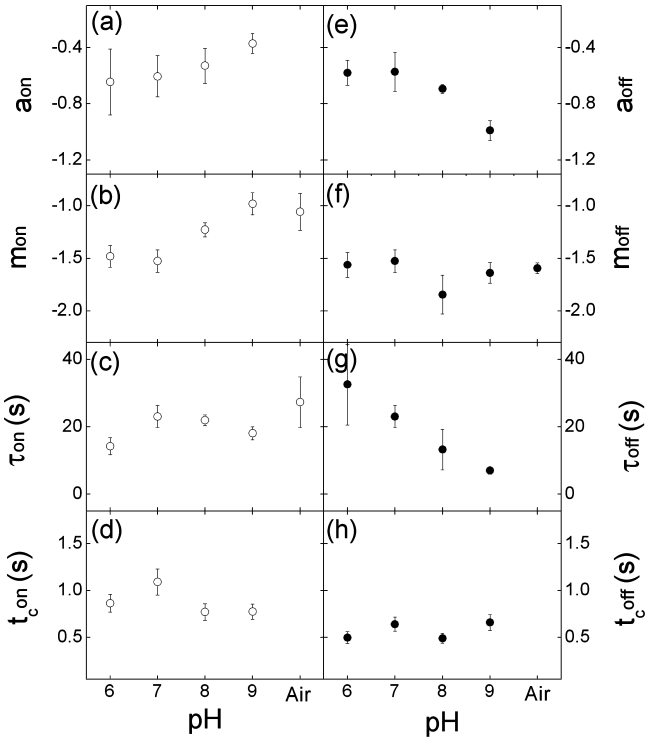

Figure 3. Extracted parameters from eqs 2 and 3 to describe the blinking dynamics (a−d) for "on" events and (e−h) for "off" events: the lower power-law slope at short time scales, *a* (a,e), the power law slope at intermediate time scales, *m* (b,f), the characteristic time describing the exponential roll-off at longer time scales, τ (c,g), and the time at which the two power law functions intersect, t_c (d,h).

with $m = -(1 + \nu)$. Theoretical studies have suggested $\nu = 0.5$, in agreement with many experimental observations showing $m \approx -1.5$.[8,12,33] Equation 1 holds only for times longer than a critical time, t_c, below which it takes the form[12,33]

$$P(t) \propto t^a \quad \text{for } t \ll t_c \tag{2}$$

where $a = -(1 - \nu)$. A value of t_c in the range of ~5−35 ms was recently found experimentally for QDs in air.[16] However, it was discussed that t_c varied from sample to sample. Finally, the probability density function often shows an exponential damping tail at long times,[2,8,9,12,33] leading to an extension of eq 1 to the form

$$P(t) \propto t^m \exp(^{-t}/_{\tau}) \quad \text{for } t \gg t_c \tag{3}$$

where τ is the characteristic time of the exponential tail.

We have fit our experimental data to eqs 2 and 3 for the short time scales ($<t_c$) and the long time scales ($>t_c$), respectively, and extracted four parameters for both "on" and "off" time distributions: the lower power-law slope at short time scales, $a = -(1- \nu)$, the power-law slope at intermediate time scales, $m = -(1+\nu)$, the characteristic time describing the exponential roll off at longer time scales, τ, and the time at which the two power-law functions intersect, t_c. An example fit is shown for pH 6 in Figure 2. Due to the log scales, in order that the data at low probability are able to be adequatley fit, the χ^2 values of the low probability data are logarithmically weighted accordingly (*i.e.*, the data are fit by linearizing the log scale; see Heyes *et al.*).[9] All pH data were fit in the same way and were of similar quality. The extracted parameters for all samples (including in air) are presented in Figure 3a−d for "on" times and Figure 3e−h for "off" times. The decrease in "on" times duration and increase in "off" times duration evident from Figure 2 are manifest in the extracted fit parameters as follows: For "on" times, the power law slope, *m*, increases in steepness from −1 at pH 9 to −1.5 at pH 6, whereas it is approximately constant at −1.6 for "off" times over the same pH range. The power-law slope, *a*, becomes more negative (steeper) for "on" times and less negative (flatter) for "off" times as pH is lowered. The characteristic time describing the exponential roll-off, τ, increases for "off" times as pH is lowered, but remains relatively constant for "on" times between pH 9 and 6. Finally, the extracted t_c value describing the critical time at which the power-law behavior changes slope shows no systematic variation over the pH range studied for both "on" and "off" times, varying between 500 ms and 1 s. However, t_c tends to be slightly lower for "off" times as compared to "on" times. In air, no change in power-law slope is observed at shorter time scales for both "on" and "off" times, and thus both *a* and t_c are not extracted. Furthermore, the "off" times did not show the exponential roll-off in air, in agreement with previous data,[1,2,5,6,9,16,34,35] which estimated τ_{off} to be on the thousand second time scale for a QD sample dried in air.[35]

We also performed the same experiments on uncapped CdSe QDs (consisting of only a CdSe core and TOPO/HDA ligands). In general, the results agree very well with those of the core−shell QDs. The detailed data are given as Supporting Information in Figure S2. Specifically, an increase in the dark fraction is observed as pH is lowered from 9 to 6. However, the effect was significantly stronger for uncapped QDs than for core−shell QDs. This result is expected due to the lack of a protective shell layer which offers some shielding of the CdSe core. Furthermore, there is already a large difference in the blinking statistics between pH 9 buffer and air, suggesting that a concentration of H^+ of 10^{-9} M is already sufficient to produce a strong effect. This observation is in contrast to the core−shell QDs, which show very similar results for the air and the pH 9 buffer samples (Figure 1). Upon addition of pH 9 buffer, the "on" times decrease and the "off" times increase significantly. Lowering to pH 8 causes an additional slight change, but it is apparent that the effect of H^+ ions is practically saturated at pH 9. On the other hand, the presence of the shell in the core−shell QDs requires a lower pH in order to see the same magnitude of change (Figure 2). For the uncapped QD samples, image time

series at pH values lower than 8 contained too few fluorescent QDs to allow a statistically significant analysis. Therefore, no further analysis was performed for the uncapped QDs. In any case, the results on uncapped CdSe QDs support our results on core−shell QDs which suggest a H^+-induced effect on both the dark fraction and the blinking statistics.

The fact that the core−shell QDs did show an effect on the observed dark fraction and blinking as a function of pH was initially a surprising result. This prompted us to perform a TEM characterization of the sample to determine the morphology and homogeneity of the ZnS shell. An example image is presented in Figure S3 in the Supporting Information, which clearly shows that the ZnS shell is highly inhomogeneous and rod-like in shape. Non-uniform shell growth is often observed and has been characterized in the literature.[36−39] There is a wide distribution of shell thickness and morphology both within a single QD and for different nanoparticles, which clearly does not offer optimal uniform protection of the CdSe core from the external environment. Thin sections of the shell (or small holes in the shell layer) would allow H^+ ions to interact with the CdSe core, which would affect their fluorescence properties, and this is supported by our observations.

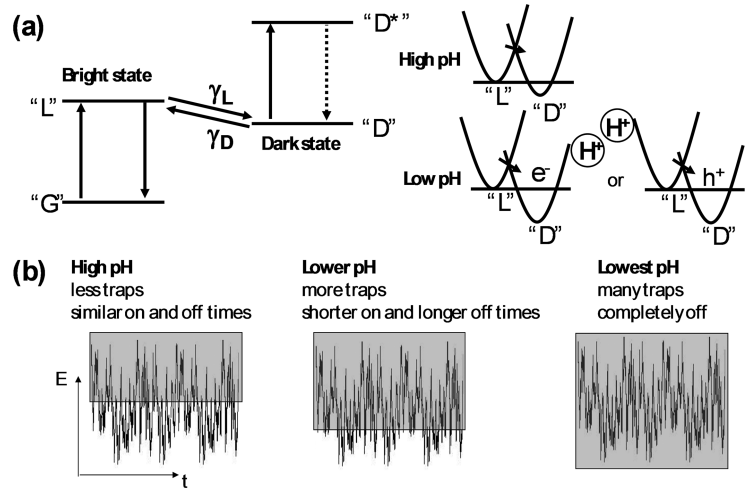

Figure 4. Models describing the effects of pH on the blinking statistics and the dark fraction. (a) Using the Tang−Marcus model,[12,33] blinking is described as a diffusive transition between a bright state and a dark state on a potential energy surface. The possible effects of H^+ ions are presented to explain our observations of increased "off" times and decreased "on" times with decreasing pH. (b) Using the Frantsuzov−Marcus model,[8] blinking is described as diffusion of the transition energy between the $1S_e$ and the $1P_e$ conduction band electronic energy levels which cross a transition region between being in (shaded area) and out of (nonshaded area) resonance with the energy difference between the $1S_{3/2}$ valence band hole state and a number of hole trap states lying deep in the band gap. Increasing the number of hole trap states (and/or decreasing their energy relative to the $1S_{3/2}$) will cause a reduced crossing probability, thereby increasing the "off" times and decreasing the "on" times duration.

DISCUSSION

The coupled observation of changing of the blinking statistics and the dark fraction of the QDs as a function of pH suggests that the mechanisms underlying these effects are related. The variation in power-law exponent and exponential bending tail was discussed theoretically by Tang and Marcus.[12,33] In their model, the power-law exponent, m, for "on" and "off" times was related to the diffusion of rate constants for the transitions from the bright state to the dark state, γ_L and γ_D, respectively, shown in Figure 4a. Our data suggest that m_{on} varies with pH but that m_{off} remains relatively constant (Figure 3). In the framework of the Tang−Marcus model,[12,33] this is consistent with γ_L being affected by pH but γ_D not. If the ratio of γ_L to γ_D is large enough, the QD will spend the majority of its time in the dark state, "D", keeping the QD "off" and effectively increasing the observed dark fraction. In the same model, the exponential cutoff tail was related to the depth of the potential well of the dark state, "D", relative to the bright state, "L". A deeper potential well for "D" relative to "L" would increase the probability of observing longer "off" times resulting in an increase in τ_{off}. Our observation that decreasing the pH causes an increase in the τ_{off} is consistent with greater number of H^+ ions reducing the depth of the "D" state potential well relative to "L". A possible explanation for this observation may be related to the presence of H^+ ions at the surface either assisting the trapping of an electron adjacent to it or trapping a hole at the opposite side of the QD due to Coulomb repulsion (Figure 4a), thereby reducing the depth of "D" relative to "L". Changing the depth of "D" relative to "L" should also change the relative slopes at the intersection of the two states. In particular, the presence of external positive charges such as H^+ ions has been shown to affect the electron and hole wave functions,[27] and one would expect them to change the shape of the potential wells of "D" and/or "L". Thus, the H^+ ions would affect the intersection between these states. Since m_{on} and m_{off} are related to diffusion on these potential energy surfaces, it is not surprising that pH affects m_{on} and/or m_{off}. The presence of an electric field was shown to influence the spectral diffusion in QDs due to rearrangement of charges within the QD,[40] which is also consistent with our hypothesis. Our observation of the change in m_{on} with pH implies that the H^+ ion affects the "L" to "D" transition more than the "D" to "L" transition, which would mean that the H^+ ion interacts more strongly with "L". This is consistent with the "D" state being a hole trap rather than an electron trap state. This hole-trapping mechanism is also in accordance with the Auger-assisted hole-trapping model proposed by Frantsuzov and Marcus, highlighting the coupled nature of these two models.[8]

An alternative explanation of the pH effect on blinking and dark fraction would be that H^+ ions cause a chemical change at the QD surface, which increases the number of hole trap states (and/or reduces their energy). In the framework of the Frantsuzov−Marcus

diffusion-controlled Auger-assisted hole-trapping model,[8] such an effect is described by an increase in the width of the shaded area, as shown in Figure 4b, thereby increasing the time in which the transition energy between the hole trap states and the $1S_{3/2}$ valence band state remains in resonance with the transition energy from the $1S_e$ to the $1P_e$ excited electronic state (the QD is in the "off" state). If the number of trap states increases sufficiently (and/or the energies of the trap states are lowered enough), the resonance condition will always be met, and the QD will always be dark—thus increasing the dark fraction. Naturally, one would expect that the number and/or position of trap states follows a certain distribution over the QD ensemble at a given pH. As pH is lowered, more trap states are formed, which leads to a shift in the distribution so that, on average, as pH decreases, one first observes longer "on" times then shorter "on" times (longer "off") and finally completely "off". It should be noted here that these results have shown that the OH^- ions at high pH have little effect on blinking but that the effects increase as pH is lowered, suggesting that it is specifically the H^+ ions that are responsible for the observations. We assume that the H^+ ions cause these effects by interaction with the QD surface, but it should be clarified that we show no direct evidence of H^+ ions at the QD surface. It may be possible that, if other small ions were to interact with the QD surface, they could cause a similar effect. However, our initial experiments with varying NaCl concentration showed little effect. A possible reason for this is that the Na^+ and Cl^- ions may be too large to cause an effect on the core through the shell material. Future investigations on the effect of other small positive ions are necessary to make any further conclusions.

The tendency for the QDs to be less bright in the "on" state as pH is lowered (Figure 1e) is in agreement with *ab initio* calculations performed by Wang.[27] The calculations showed that the presence of a charge close to the surface of the QD affects the overlap of the electron and hole wave functions in the "on" state, thereby reducing the fluorescence intensity.[27] Our data in Figure 1e provide experimental evidence for these calculations and support our hypothesis that H^+ ions indeed interact with the QD core. Furthermore, the observation of a decrease in "on" state intensity between air and pH 9 shows that the intensity is already affected by the presence of 10^{-9} M H^+ ions. However, as described above, the blinking is not yet affected at this pH for core−shell QDs (but the same does not hold for uncapped QDs, evident from the difference in blinking between air and pH 9, Figure S1 in Supporting Information). Then, as more H^+ ions are added, the blinking dynamics begins to be affected and finally, when a certain number of H^+ ions interact with the core, the QD enters a permanent "off" state.

We have also observed the change in power-law slope at shorter time scales as was recently observed by Pelton *et al.*[16] However, the value of t_c found for the QD samples measured in this study is on the 500 ms to 1 s time scale, about 2 orders of magnitude longer than the QD samples measured by Pelton *et al*. Other experiments on the 0.2 ms time scale did not show a change in the power-law slope,[3] as did experiments on the nanosecond time scale.[17] It has been previously discussed that the value of t_c may depend on a variety of parameters such as sample preparation, temperature, excitation intensity, and environmental conditions. We found a t_c on the 500 ms to 1 s time scale only for samples exposed to the pH buffers, but not for samples dried in air. This t_c observation was true for both the core−shell QDs and uncapped QDs under the same experimental conditions, suggesting that the exact nature of the experimental conditions may play a larger role in determining t_c than the actual sample preparation does. Most previous QD blinking experiments have been performed on either QDs dried in air or encapsulated within polymers,[1,2,5,6,9,16,34] and the only evidence of t_c under these conditions was found on much shorter time scales (~5−35 ms).[16] It appears that the presence of solution (solvent and/or solute) molecules increases t_c from the several millisecond time scale to the several hundred millisecond time scale. The slightly lower value of t_c for "off" times compared to "on" times for these samples may be related to the idea that the presence of interacting species (*e.g.*, solvent and/or solute) affects diffusion on the potential energy surface of the bright state more than the dark state, also in agreement with the fact that m_{on} changes more than m_{off}. However, more experiments are necessary to pinpoint the exact determinants of t_c.

In conclusion, we have observed that solution pH affects both the blinking dynamics and the dark fraction of QDs in a systematic way. A diffusion-controlled model may be used to describe a coupled effect of H^+ ions on blinking and dark fraction. The presence of H^+ ions affects the transition probability to a dark state either by increasing the rate of diffusion to the dark state or by increasing the number of available trap states, or both. When the diffusion rate to the trap states and/or the number of trap states increases above a certain point, the QD will always be in an "off" state, thereby increasing the dark fraction. Our experimental results support a mechanism connecting QD blinking and dark fraction *via* a diffusion-controlled model. However, other possible interpretations cannot be ruled out at the present time. Although several studies have shed doubt onto the external trap model,[9,13] other reports suggest that blinking does change with environmental factors such as the dieletric constant of the environment[6] or the addition of electron-donating species to the solution.[18,24] The external traps may also react to H^+ ions, which then may affect blinking. In core−shell

QDs with reasonably thick shells, external traps are expected to be at least several nanometers from the emitting core, so the traps should be strongly affected by pH if they do play a role in blinking. An additional interpretation on blinking was provided by Dutta *et al.* with the hypothesis that fluctuations in the surface charge density of double layer screening charges around the QDs can lead to power-law blinking dynamics.[41] This is only relevant for QDs in solution and not for samples dried in air or trapped in a solid matrix. However, this double layer potential fluctuation may be affected by pH and does provide a possible alternative relevant mechanism of blinking in solution to that in air or in a solid matrix. From the conflicting reports published in the literature, it is likely that a number of different mechanisms may be responsible for blinking. These results are particularly important for developing a more complete theory of QD blinking but are also relevant in various applications of QDs, especially for quantitative biological imaging applications where pH variations exist between the cytoplasmic and extracellular spaces and within organelles.[42]

MATERIALS AND METHODS

QD Samples. We used commercially available streptavidin-functionalized CdSe/ZnS quantum dots (QD605-streptavidin, Invitrogen Canada Inc., Burlington, ON) with emission wavelength centered at 605 nm. Two different batches of QDs were used to ensure that effects observed were not batch-specific. Additional experiments on uncapped CdSe QDs were performed with QDs synthesized in our laboratory (emission wavelength 605 nm) in trioctylphosphine oxide (TOPO) and hexadecylamine (HDA) and using CdO as a precursor following standard procedures.[9,43,44] All chemicals were purchased from Sigma-Aldrich (St. Louis, MO), unless otherwise stated.

Attaching QDs to Glass Coverslips. The microscope coverslips (Fisher Scientific #1) were first cleaned in Piranha solution (3:1 concentrated sulfuric acid/30% hydrogen peroxide). Glass surfaces were then amino functionalized using 2% (v/v) 3-aminopropyltriethoxylsilane (Pierce, Rockford, IL) in anhydrous acetone. The amino groups were next modified with a 10 mM aqueous Sulfo-LC-SPDP solution (Pierce) to render the surface reactive to sulfohydryl groups. Biotinylated BSA was reduced in 50 mM DTT, exposed to the glass surface, and stored overnight at 4 °C to allow the sulfohydryl group of the BSA to covalently bind to the functionalized glass coverslip. Residual unconjugated BSA was removed from the surface by rinsing with PBS/EDTA buffer (Pierce).

The commercial QD stock solution (~2 μM) was diluted by a factor of ~100 in Milli-Q water (>18 MΩ · cm^{-1}) and sonicated for 15 min prior to deposition on the protein-coated glass coverslip. The coverslip was then rinsed with Milli-Q water to remove unbound QDs. Home-made, uncapped CdSe QDs were deposited directly from a dilute toluene solution onto a Piranha-cleaned glass coverslip. The QD solution was dried by air flow shortly after deposition to minimize the formation of aggregates on the glass caused by cohesive forces during slow drying. Since the uncapped CdSe QDs have water-insoluble ligands on their surface, they are not washed away by exposing them to aqueous pH buffer solutions, and thus covalent immobilization was unnecessary. All samples were imaged immediately after preparation.

Fluorescence Microscopy Measurement and Analysis of Single QDs. To investigate the effects of base or acid on QD fluorescence, HCl or NaOH was added to PBS buffer (Fisher Scientific, Pittsburgh, PA) to prepare solutions with pH values ranging from 9 to 5. The buffer was deposited directly on the glass coverslips to which the QDs were attached.

Image time series consisting of 2000 frames with 50 ms frame resolution of spatially resolved QDs were collected on a home-built objective-type total internal reflection fluorescence (TIRF) microscope with an intensified PentaMax charge-coupled device (CCD) camera (Princeton Instruments, Trenton, NJ) as previously described.[45] The 488 nm line from a CW Ar^+ laser (Melles Griot 35 LAP 431, Carlsbad, CA) was used for excitation through a Zeiss Planapo 100×, 1.45 NA objective lens. We adjusted the laser power to ensure that no photobleaching occurred, while achieving maximum brightness. We determined a laser power of ~0.3 mW to be optimal, which gives a power density at the sample of ~3 W · cm^{-2}. Fluorescence from the sample was collected using the same objective and filtered with an emission filter centered at 605 nm with a bandwidth of 55 nm (Chroma Technology, Rockingham, VT) and imaged onto the CCD camera.

Histogram analysis was performed as previously described,[9,34] with slight modification. A maximum intensity projection image is calculated by recording the maximum intensity of each pixel for all frames in the time series in a single projected image frame. This method allows the displayed intensity of each QD to be independent of its blinking statistics and only dependent on its maximum integrated brightness within a single frame. This image is used to calculate the number of fluorescent QDs in the sample area and, subsequently, to identify the coordinates of single QDs. The fluorescence from each QD as a function of time is extracted from the image series, a threshold is set, determined by the local background intensity, to distinguish "on" events from "off" events, and the duration of times that the QD spends in each state is calculated. This procedure is repeated for several hundred individual QDs.

Atomic Force Microscopy (AFM). AFM images were acquired using a Bioscope I with Nanoscope IIIa controller (Veeco Instruments, Woodbury, NY) operating in contact mode. The scan rate was set to 1 Hz over a total area of 5 × 5 μm^2 at 512 × 512 pixels. All images were obtained in liquid using silicon nitride tips (Veeco Instruments).

Transmission Electron Microscopy (TEM). A drop of QD solution was placed on a TEM grid (Electron Microscopy Sciences, Hatfield, PA) and left to dry in a desiccator for ~2 h. TEM images were acquired on a Philips CM200 electron microscope operating at 200 kV.

Acknowledgment. P.W.W. and P.G. acknowledge support from the Natural Sciences and Engineering Research Council of Canada (NSERC), Canadian Institutes of Health Research (CIHR), and Le Fonds Québécois de la Recherche sur la Nature et les Technologies (FQRNT). P.G. acknowledges Canadian Institute for Advanced Research (CIfAR). We thank Dr. Andrei Kobitski from the University of Ulm, Germany, for the original Matlab code used in the histogram analysis, and Behrang Sadeghi for assistance with the fitting code. We appreciate technical help from Xue-Dong Liu with the TEM imaging.

Supporting Information Available: Addional experimental data and figures. This material is available free of charge *via* the Internet at http://pubs.acs.org.

REFERENCES AND NOTES

1. Nirmal, M.; Dabbousi, B. O.; Bawendi, M. G.; Maklin, J. J.; Trautman, J. K.; Harris, T. D.; Brus, L. E. Fluorescence Intermittency in Single Cadmium Selenide Nanocrystals. *Nature* **1996**, *383*, 802–804.
2. Shimizu, K. T.; Neuhauser, R. G.; Leatherdale, C. A.; Empedocles, S. A.; Woo, W. K.; Bawendi, M. G. Blinking Statistics in Single Semiconductor Nanocrystal Quantum Dots. *Phys. Rev. B* **2001**, *63*, 205316.

3. Kuno, M.; Fromm, D. P.; Hamann, H. F.; Gallagher, A.; Nesbitt, D. J. Nonexponential Blinking Kinetics of Single CdSe Quantum Dots: A Universal Power Law Behavior. *J. Chem. Phys.* **2000**, *112*, 3117–3120.
4. Krauss, T. D.; Brus, L. E. Charge, Polarizability, and Photoionization of Single Semiconductor Nanocrystals. *Phys. Rev. Lett.* **1999**, *83*, 4840–4843.
5. Kuno, M.; Fromm, D. P.; Johnson, S. T.; Gallagher, A.; Nesbitt, D. J. Modeling Distributed Kinetics in Isolated Semiconductor Quantum Dots. *Phys. Rev. B* **2003**, *67*, 125304.
6. Issac, A; von Borczyskowski, C.; Cichos, F. Correlation between Photoluminescence Intermittency of CdSe Quantum Dots and Self-Trapped States in Dielectric Media. *Phys. Rev. B* **2005**, *71*, 161302.
7. Osad'ko, I. S. Power-Law Statistics of Intermittent Photoluminescence in Single Semiconductor Nanocrystals. *JETP Lett.* **2004**, *79*, 522–526.
8. Frantsuzov, P. A.; Marcus, R. A. Explanation of Quantum Dot Blinking without the Long-Lived Trap Hypothesis. *Phys. Rev. B* **2005**, *72*, 155321.
9. Heyes, C. D.; Kobitski, A. Y.; Breus, V. V.; Nienhaus, G. U. Effect of the Shell on Blinking Statistics in Single Core−Shell Quantum Dots—A Single Particle Fluorescence Study. *Phys. Rev. B* **2007**, *75*, 125431.
10. Verberk, R.; Oijen, A. v.; Orrit, M. Simple Model for the Power Law Blinking of Single Semiconductor Nanocrystals. *Phys. Rev. B* **2002**, *66*, 2332021–2332024.
11. Cichos, F.; von Borczyskowski, C.; Orrit, M. Power-Law Intermittency of Single Emitters. *Curr. Opin. Colloid Interface Sci.* **2007**, *12*, 272–284.
12. Tang, J.; Marcus, R. A. Mechanisms of Fluorescence Blinking in Semiconductor Nanocrystal Quantum Dots. *J. Chem. Phys.* **2005**, *123*, 054704.
13. Pelton, M.; Grier, D. G.; Guyot-Sionnest, P. Characterizing Quantum-Dot Blinking Using Noise Power Spectra. *Appl. Phys. Lett.* **2004**, *85*, 819–821.
14. Chen, Y.; Vela, J.; Htoon, H.; Casson, J. L.; Werder, D. J.; Bussian, D. A.; Klimov, V. I.; Hollingsworth, J. A. "Giant" Multishell CdSe Nanocrystal Quantum Dots with Suppressed Blinking. *J. Am. Chem. Soc.* **2008**, *130*, 5026..
15. Mahler, B.; Spinicelli, P.; Buil, S.; Quelin, X.; Hermier, J. P.; Dubertret, B. Towards Non-Blinking Colloidal Quantum Dots. *Nat. Mater.* **2008**, *7*, 659–664.
16. Pelton, M.; Smith, G.; Scherer, N. F.; Marcus, R. A. Evidence for a Diffusion-Controlled Mechanism for Fluorescence Blinking of Colloidal Quantum Dots. *Proc. Natl. Acad. Sci. U.S.A.* **2007**, *104*, 14249–14254.
17. Sher, P. H.; Smith, J. M.; Dalgarno, P. A.; Warburton, R. J.; Chen, X.; Dobson, P. J.; Daniels, S. M.; Pickett, N. L.; O'Brien, P. Power Law Carrier Dynamics in Semiconductor Nanocrystals at Nanosecond Timescales. *Appl. Phys. Lett.* **2008**, 92.
18. Hohng, S.; Ha, T. Near-Complete Suppression of Quantum Dot Blinking in Ambient Conditions. *J. Am. Chem. Soc.* **2004**, *126*, 1324–1325.
19. Heuff, R. F.; Marrocco, M.; Cramb, D. T. Saturation of Two-Photon Excitation Provides Insight into the Effects of a Quantum Dot Blinking Suppressant: A Fluorescence Correlation Spectroscopy Study. *J. Phys. Chem. C* **2007**, *111*, 18942–18949.
20. Jeong, S.; Achermann, M.; Nanda, J.; Ivanov, S.; Klimov, V. I.; Hollingsworth, J. A. Effect of the Thiol-Thiolate Equilibrium on the Photophysical Properties of Aqueous CdSe/ZnS Nanocrystal Quantum Dots. *J. Am. Chem. Soc.* **2005**, *127*, 10126–10127.
21. Breus, V. V.; Heyes, C. D.; Nienhaus, G. U. Quenching of CdSe−ZnS Core−Shell Quantum Dot Luminescence by Water-Soluble Thiolated Ligands. *J. Phys. Chem. C* **2007**, *111*, 18589–18594.
22. Fomenko, V.; Nesbitt, D. J. Solution Control of Radiative and Nonradiative Lifetimes: A Novel Contribution to Quantum Dot Blinking Suppression. *Nano Lett.* **2008**, *8*, 287–293.
23. Early, K. T.; McCarthy, K. D.; Hammer, N. I.; Odoi, M. Y.; Tangirala, R.; Emrick, T.; Barnes, M. D. Blinking Suppresion and Intensity Recurrences in Single CdSe−Oligo(phenylene vinylene) Nanostructures: Experiment and Kinetic Model. *Nanotechnology* **2007**, *18*, 424027.
24. Biebricher, A.; Sauer, M.; Tinnefeld, P. Radiative and Nonradiative Rate Fluctuations of Single Colloidal Semiconductor Nanocrystals. *J. Phys. Chem. B* **2006**, *110*, 5174–5178.
25. Khatchadourian, R.; Bachir, A.; Clarke, S. J.; Heyes, C. D.; Wiseman, P. W.; Nadeau, J. L. Fluorescence Intensity and Intermittency as Tools for Following Dopamine Bioconjugate Processing in Living Cells. *J. Biomed. Biotechnol.* **2007**, *2007*, 70145.
26. Zhang, K.; Chang, H.; Fu, A.; Alivisatos, A. P.; Yang, H. Continuous Distribution of Emission States from Single CdSe/ZnS Quantum Dots. *Nano Lett.* **2006**, *6*, 843–847.
27. Wang, L.-W. Calculating the Influence of External Charges on the Photoluminescence of a CdSe Quantum Dot. *J. Phys. Chem. B* **2001**, *105*, 2360–2364.
28. Ebenstein, Y.; Mokari, T.; Banin, U. Fluorescence Quantum Yield of CdSe/ZnS Nanocrystals Investigated by Correlated Atomic-Force and Single-Particle Fluorescence Microscopy. *Appl. Phys. Lett.* **2002**, *80*, 4033–4035.
29. Owen, R. J.; Heyes, C. D.; Knebel, D.; Röcker, C.; Nienhaus, G. U. An Integrated Instrumental Setup for the Combination of Atomic Force Microscopy with Optical Spectroscopy. *Biopolymers* **2006**, *82*, 410–414.
30. Yao, J.; Larson, D. R.; Vishwasrao, H. D.; Zipfel, W. R.; Webb, W. W. Blinking and Nonradiant Dark Fraction of Water-Soluble Quantum Dots in Aqueous Solution. *Proc. Natl. Acad. Sci. U.S.A.* **2005**, *102*, 14284–14289.
31. Berciaud, S.; Cognet, L.; Lounis, B. Photothermal Absorption Spectroscopy of Individual Semiconductor Nanocrystals. *Nano Lett.* **2005**, *5*, 2160–2163.
32. Brokmann, X.; Coolen, L.; Dahan, M.; Hermier, J. P. Measurement of the Radiative and Nonradiative Decay Rates of Single CdSe Nanocrystals through a Controlled Modification of Their Spontaneous Emission. *Phys. Rev. Lett.* **2004**, *93*, 107403.
33. Tang, J.; Marcus, R. A. Diffusion-Controlled Electron Transfer Processes and Power-Law Statistics of Fluorescence Intermittency of Nanoparticles. *Phys. Rev. Lett.* **2005**, *95*, 107401.
34. Kobitski, A. Y.; Heyes, C. D.; Nienhaus, G. U. Total Internal Reflection Fluorescence Microscopy—A Powerful Tool to Study Single Quantum Dots. *Appl. Surf. Sci.* **2004**, *234*, 86–92.
35. Chung, I.; Bawendi, M. G. Relationship between Single Quantum-Dot Intermittency and Fluorescence Intensity Decays from Collections of Dots. *Phys. Rev. B* **2004**, *70*, 165304.
36. Dabbousi, B. O.; Rodriguez-Viejo, J.; Mikulec, F. V.; Heine, J. R.; Mattoussi, H.; Ober, R.; Jensen, K. F.; Bawendi, M. G. (CdSe)ZnS Core−Shell Quantum Dots: Synthesis and Optical and Structural Characterization of a Size Series of Highly Luminescent Materials. *J. Phys. Chem. B* **1997**, *101*, 9463–9475.
37. Baranov, A. V.; Rakovich, Y. P.; Donegan, J. F.; Perova, T. S.; Moore, R. A.; Talapin, D. V.; Rogach, A. L.; Masumoto, Y.; Nabiev, I. Effect of ZnS Shell Thickness on the Phonon Spectra in CdSe Quantum Dots. *Phys. Rev. B* **2003**, *68*, 165306.
38. Borchert, H.; Talapin, D. V.; McGinley, C.; Adam, S.; Lobo, A.; de Castro, A. R. B.; Moller, T.; Weller, H. High Resolution Photoemission Study of CdSe and CdSe/ZnS Core−Shell Nanocrystals. *J. Chem. Phys.* **2003**, *119*, 1800–1807.
39. Yu, Z.; Guo, L.; Du, H.; Krauss, T.; Silcox, J. Shell Distribution on Colloidal CdSe/ZnS Quantum Dots. *Nano Lett.* **2005**, *5*, 565–570.
40. Empedocles, S. A.; Bawendi, M. G. Quantum-Confined Stark Effect in Single CdSe Nanocrystallite Quantum Dots. *Science* **1997**, *278*, 2114–2117.

41. Dutta, M.; Stroscio, M. A.; Vasudev, M.; Ramadurai, D.; Torres, L.; West, B. J. Blinking Mechanism of Colloidal Semiconductor Quantum Dots: Blinking Mechanisms. *J. Comput. Electron.* **2007**, *6*, 301–304.
42. Sun, Y. H.; Liu, Y. S.; Vernier, P. T.; Liang, C. H.; Chong, S. Y.; Marcu, L.; Gundersen, M. A. Photostability and pH Sensitivity of CdSe/ZnSe/ZnS Quantum Dots in Living Cells. *Nanotechnology* **2006**, *17*, 4469–4476.
43. Talapin, D. V.; Rogach, A. L.; Kornowski, A.; Haase, M.; Weller, H. Highly Luminescent Monodisperse CdSe and CdSe/ZnS Nanocrystals Synthesized in a Hexadecylamine-Trioctylphosphine Oxide-Trioctylphospine Mixture. *Nano Lett.* **2001**, *1*, 204–211.
44. Peng, Z. A.; Peng, X. Formation of High-Quality CdTe, CdSe, and CdS Nanocrystals Using CdO as Precursor. *J. Am. Chem. Soc.* **2001**, *123*, 183–184.
45. Bachir, A.; Durisic, N.; Hebert, B.; Grütter, P.; Wiseman, P. W. Characterization of Blinking Dynamics in Quantum Dot Ensembles Using Image Correlation Spectroscopy. *J. Appl. Phys.* **2006**, *99*, 064503.